Zihui XIA and Fernand ELLYIN

Constitutive Modeling for Elastoplastic Materials under Nonproportional Cyclic Loading

Department of Mechanical Engineering, University of Alberta Edmonton, Alberta, Canada,

Keywords: constitutive model, plasticity, nonproportional cyclic loading, finite element software

ABSTRACT: A comprehensive elastoplastic constitutive model is described. This model is capable of simulating and predicting materials' response to complex cyclic loading paths and histories including transient hardening or softening, ratcheting, rate-dependency, etc. The model has been formulated and programmed in a finite element format which can be used in combination with the general ADINA code, as a user defined material model. It can also be inserted in any other commercial finite element code which has an option for a user-defined material model. Numerous examples involving different types of nonproportional cyclic loading cases have been calculated by using this program. The results clearly show that this model is far superior to the elastoplastic material models currently available in the commercial finite element analysis codes.

Introduction

In most commercial finite element analysis codes the elastic-plastic material models are the classical isotropic or kinematic hardening rules[1,2]. For proportional monotonic loading the two models give the same result. However for cases which include reversed plastic loading or cyclic loading, neither model can provide a suitable prediction of materials' behaviour. A Mróz type modelb [3] has been introduced in the ADINA program, which provides a more reasonable prediction for relatively simple cyclic loadings. For more complex non-proportional cyclic loadings there is still need for further work.

Strain energy based criteria are often adopted in biaxial/multiaxial fatigue theories[4]. The advantage of an energy parameter to either stress or strain criterion is that the path-dependency of material behaviour is inherent in the energy parameters. Therefore, various proportional and nonproportional cyclic loading paths can be differentiated in an energy criterion. To use and calculate the energy parameters, a proper constitutive model (stress-strain relationship) is required.

A hierarchy of elastic-plastic constitutive models which includes rate-independent, rate-dependent and finite deformation formulations has been developed in recent years by the present authors[5-7]. To facilitate the practical application, the rate-independent and rate-dependent models have been programmed into a package of user defined model which can be used in combination with the ADINA computer code among others. The performance and validation of the model are verified by numerous examples involving different types of loading paths and histories. The predicted results are compared with the experimental data. It is shown that this model has definite advantages compared to those currently available, yet it is relatively simple to implement.

Description of the Constitutive Model

Our model is developed based on the classical incremental plastic theories. Three basic principles, i.e., the decomposition of total strain increments into elastic and plastic parts, the generalized Hook's law for the elastic strain increment, and the associated flow rule relating the plastic strain increment to a von Mises yield surface, are adopted in conformity with the classical approach. They are expressed as,

$$d\varepsilon_{ij}^{t} = d\varepsilon_{ij}^{e} + d\varepsilon_{ij}^{p} \tag{1}$$

$$d\varepsilon_{ij}^{e} = \frac{1}{E}[(1+\nu)\delta_{ik}\delta_{jl} - \nu\delta_{ij}\delta_{kl}]d\sigma_{kl} \tag{2}$$

$$d\varepsilon_{ij}^{p} = \frac{9}{4q^2}\left(\frac{1}{E_t} - \frac{1}{E}\right)\bar{s}_{ij}\bar{s}_{kl}d\sigma_{kl} \tag{3}$$

Where E is the elastic modulus, E_t is the instantaneous tangent modulus, ν is Poisson's ratio, δ_{ij} is the Kronecker delta, and $\bar{s}_{ij} = \bar{\sigma}_{ij} - \delta_{ij}\sigma_{kk}/3$ and $\bar{\sigma}_{ij} = \sigma_{ij} - \alpha_{ij}$, with other symbols defined below.

Main features of the constitutive model

The proposed model is based on two surfaces in the stress space. In addition to the yield surface, a stress memory surface is also defined. These two surfaces are expressed by,

$$\phi_y = f_y(\sigma_{ij} - \alpha_{ij}) - q^2 = 0 \tag{4}$$

$$\phi_m = f_m(\sigma_{ij} - \beta_{ij}) - R^2 = 0 \tag{5}$$

where α_{ij} and β_{ij} locate the center of each surface and q and R are their respective radius. A salient feature of the model is that two types of plastic loading are distinguished by the introduction of the stress memory surface. The first type is called monotonic loading (ML) in which the stress memory surface expands with the movement of the yield surface and the two surfaces remain tangent to each other. The second type is termed plastic reloading (RL). For this case the plastic deformation takes place after an elastic unloading and the current stress point is inside the stress memory surface. The evolution rules for α_{ij}, β_{ij} (eqs. 4,5) and calculation of tangent modulus E_t (eq. 3) are different for the two cases of plastic loading. The necessity of using different hardening rules for monotonic and reversed loading was pointed out by Philips[8] based on a review of experimental work. This is obviously a critical point for properly simulating a material's behaviour under cyclic loading. Detailed evolution equations for the yield surface and the calculation of E_t for the two different plastic loading cases are provided in ref.[5], and will not be repeated here.
The transient hardening or softening are reflected in change of the size of yield surface radius, q and the tangent modulus, E_t. Such changes are described by the evolution of uniaxial stress-strain curve from a virgin state with q_o, $E_{t,o}$ to a stable state with q_{st}, $E_{t,st}$. The evolution rule is given by,

$$\frac{\partial q}{\partial l_p} = \xi(q_{st} - q) \qquad \frac{\partial E_t}{\partial l_p} = \xi(E_{t,st} - E_t) \tag{6}$$

where $l_p=\int(2\, d\varepsilon^p_{ij}\, d\varepsilon^p_{ij}/3)^{1/2}$ is the accumulated plastic strain, and ξ is a material constant.

Ratcheting (cyclic creep) behaviour of materials could be very complex depending on the cyclic loading path and history. The modeling of such a behaviour still poses a challenge for various proposed constitutive models. In the present model, an evolution rule for the centre of the stress memory surface is introduced,

$$\frac{\partial \beta_{ij}}{\partial l_p} = \varsigma(\beta_{ij,st} - \beta_{ij}) \tag{7}$$

where $\beta_{ij,st}$ is the stable position of β_{ij}. For most cyclic loading paths, the mean stress point (geometric center of the cyclic stress path) could be chosen as the stable value of β_{ij}. ⌘ is generally a function of l_p. However it could be assumed to be a constant if only short term ratcheting strain for decades of cycles needs to be predicted. It is to be noted that equation (7) only applies to the RL loading case. For the ML loading case, the β_{ij} does not change and only the radius R expands. By the introduction of this relatively simple evolution rule for the memory surface, most of the complex multiaxial ratcheting behaviours of materials can be properly simulated. A comprehensive assessment of the capability of model to predict ratcheting behaviour is to be found in ref. [9].

Extension to rate-dependent model

While retaining its basic structure, the above rate-independent constitutive model has been further extended to a rate-dependent version[6]. It is assumed that the size of the yield surface is not only dependent on the history parameter, l_p, but also on the strain-rate, i.e.

$$q = q(l_p, \dot{\varepsilon}_{eq}) \tag{8}$$

in which $\dot{\varepsilon}_{eq} = (2\dot{e}_{ij}\dot{e}_{ij}/3)^{1/2}$ and $\dot{e}_{ij}$ is the deviatotic strain-rate. Incorporating the conventional logarithmic strain-rate dependency, we may express:

$$q^i = q^0\left[1 + C\log(\dot{\varepsilon}^i_{eq} / \dot{\varepsilon}^0_{eq})\right] \tag{9}$$

where C is a material constant and q^i is the value of q at a strain-rate, $\dot{\varepsilon}^i_{eq}$, and q^o is the corresponding value at a reference strain-rate, $\dot{\varepsilon}^0_{eq}$.

The change of q and E_t are now described by the evolution of a family of uniaxial curves (Fig. 1). Each uniaxial curve in the family corresponds to a fixed strain-rate, ε^i_{eq} and the curves evolve from the virgin state to a stable state with the increasing l_p, i.e.,

$$\frac{\partial q^i}{\partial l_p} = \xi(q^i_{st} - q^i), \quad \frac{\partial E^i_t}{\partial l_p} = \xi(E^i_{t,st} - E^i_t) \tag{10}$$

By introducing the above rate-dependent relationships in the constitutive model, most of the rate-dependent effects observed in the experiments can now be simulated. It is to be noted that the creep and relaxation are dealt with by another set of equations [10]. The interaction between the creep and plastic deformation is included in the two sets of constitutive equations described in [6,10].

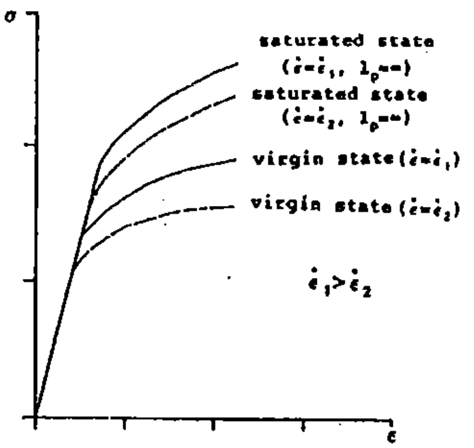

Fig.1. Family of uniaxial stress-strain curves corresponding to various strain-rates and l_p

Implementation into the user-supplied material model of ADINA

The option for user-supplied model in ADINA finite element code provides the flexibility for users to program their own constitutive model into subroutines. Both rate-independent and rate-dependent models described above have been programmed and connected with the main program of ADINA. The required input data are material constants (E, ν, ξ, ζ, C, etc.) and a family of stress-strain curves in the form of interpolation tables. For the rate-independent version, two curves are required (virgin and stable curves). At least four curves are required for the rate-dependent, two at a reference rate, usually at a very slow rate (quasi-static loading), and the other two at a higher strain-rate, see Fig.1. Any curves with a strain-rate between the two can be produced by an interpolation scheme. The uniaxial curves are updated whenever there is a switch from the elastic to plastic loading according to the value of l_p at that instance. The value of E_t in plastic loading thereafter will be calculated based on these updated curves and the current strain-rate. Proper criteria are specified in the program to distinguish three different loading cases, i.e. the elastic loading, the two types of plastic loading, ML and RL, as described in the above.

Some bench mark examples

A fairly large number of examples of a discriminating nature have been solved by using the present user-supplied model. Only a few are presented in this paper.

Transient nonproportional cyclic responses

Figures 2 shows the test and predicted results of type 304 stainless steel under a "butterfly" shape nonproportional strain cycling path in axial and torsional strain space. The test results are taken from ref. [11]. It could be seen that the model predictions are in good agreement with the experimental data.

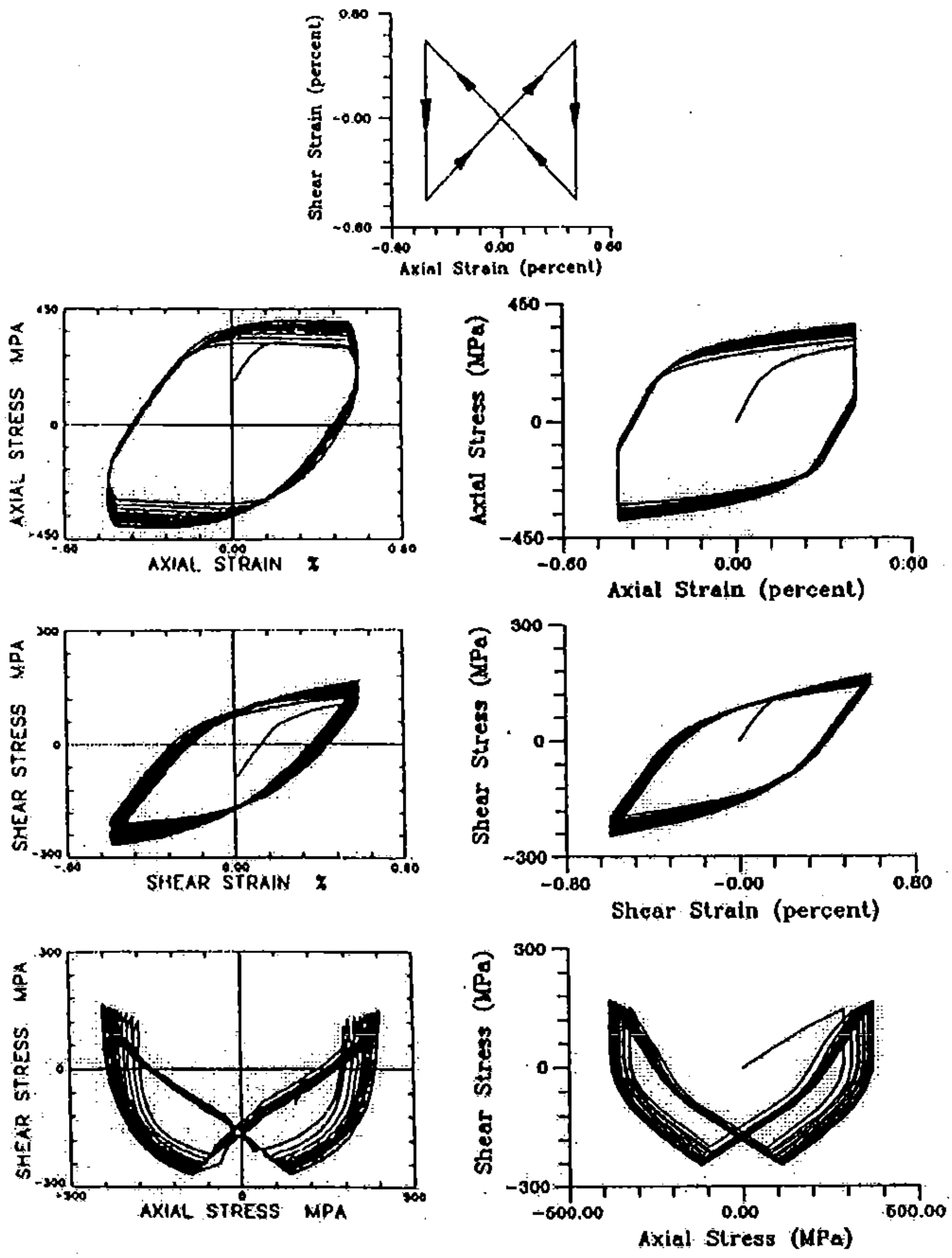

Fig.2. Transient nonproportional cyclic test of 304 stainell steel. Butterfly type cyclic strai path. Left: test result, after McDowell [11]; right: predict result. Additional strain-hardening due to nonproportional loading paths

Figures 3 shows strain-stress hysteresis loops of ASTM A-516 Gr. 70 steel subjected to biaxial strain-controlled cyclic loads with three different phase angles[12]. It is worth mentioning that while the maximum equivalent strain decreases with the increase of the phase angle($\varepsilon_{eq,max}$=0.003, 0.0028 and 0.0021, respectively), the maximum equivalent stress increases with the increasing $\sigma_{eq,max}$=233 MPa, 249 MPa and 265 MPa, respectively), see Fig. 4. This indicates an additional stain-hardening due to the nonproportionality of the strain path. The predicted strain-stress loops by the present model are shown in Fig. 3 with dotted lines. The agreement with the experimental data is indeed very good.

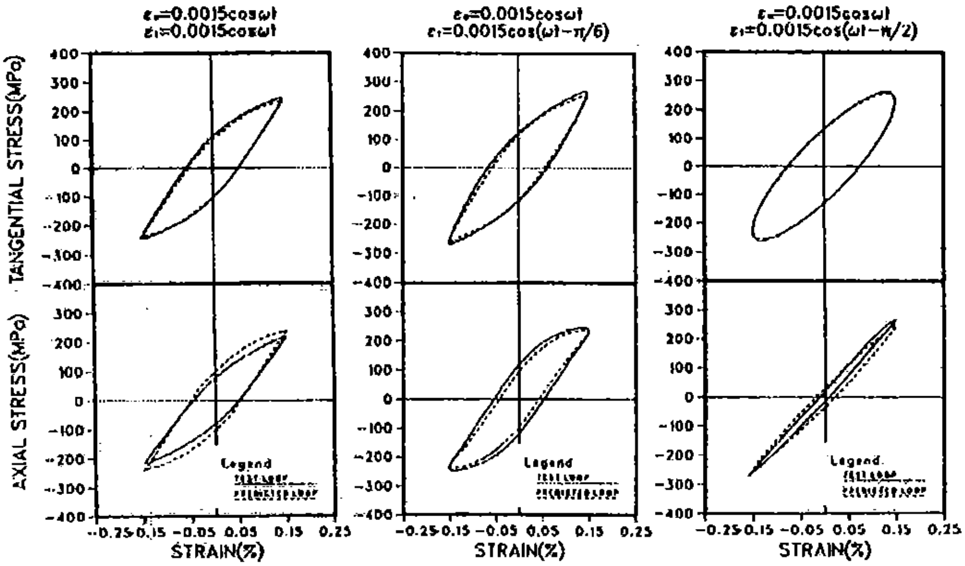

Fig.3. Hysteresis stress-strain loops for different phase angles with same strain amplitude. Solid line: test results; dotted line: predicted results.

Elliptical-shaped cyclic loading with mean compressive stress

The elliptical-shaped loading path (Fig. 5a) represents a typical nonproportional loading with a mean compressive axial stress. From the test results [13], Fig. 5b, one can observe that a negative ratcheting strain accumulates in the axial direction due to the compressive mean stress but none in the shear direction. The numerical prediction provides a very similar result, and is shown in Fig. 5c up to 1024 cycles.

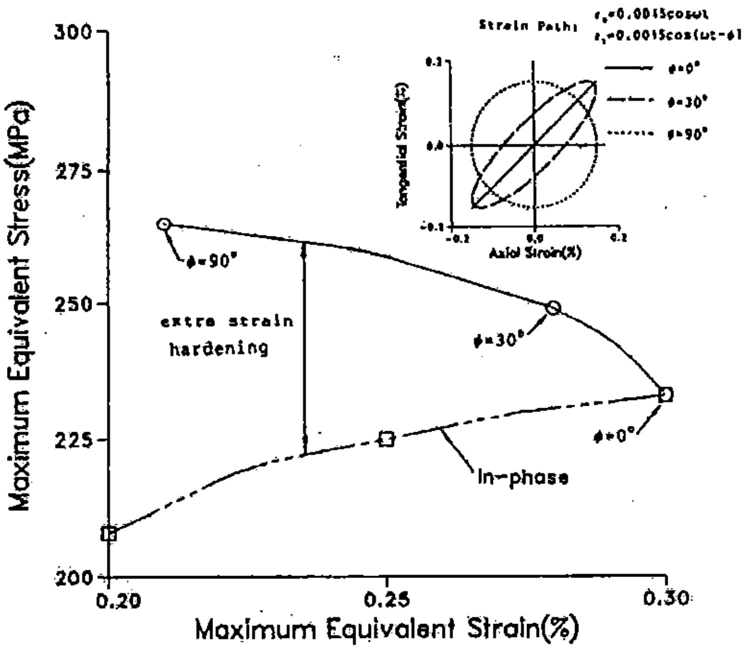

Fig.4. Extra strain hardening due to nonproportional loading

Predicting the behaviour of a composite material by a unit-cell analysis

The properties of composite materials are generally predicted by using finite element analysis of a representative unit-cell model. Here we present an example of 6061 aluminum alloy reinforced with 20% volume fraction of alumina particles [14]. The unit-cell model is a cube with a spherical alumina inclusion. The finite element model contains 1613 nodes and 1296 three-dimensional hexahedral elements, Fig. 6a. For the matrix and the inclusion the properties of 6061 aluminum alloy (elastoplastic) and alumina (elastic) were specified. The overall response of the particle-reinforced metal matrix composite is then predicted by the FEM analysis. Figure 6b shows the applied 90° out-of-phase cyclic strain path. The experimental results and numerical predictions of the composite material are shown in Fig. 6c. It is seen that the predicted results are in good agreement with the experimental data.

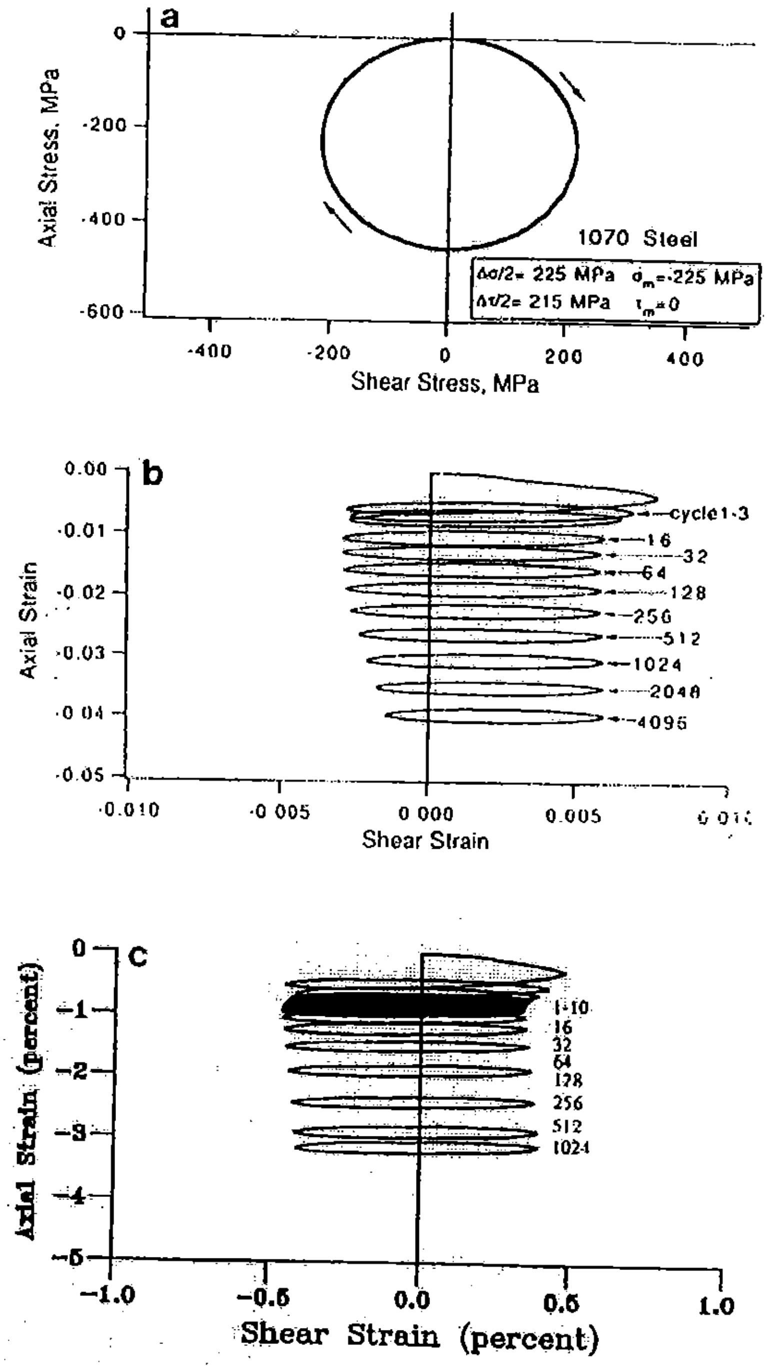

Fig.5. Elliptical-shaped cyclic loading with mean compressive stress. a: applied biaxial cyclic stress path; b: axial strai-shear loops, test result, after Jiang [13]; c: predicted results, up to 1024 cycles

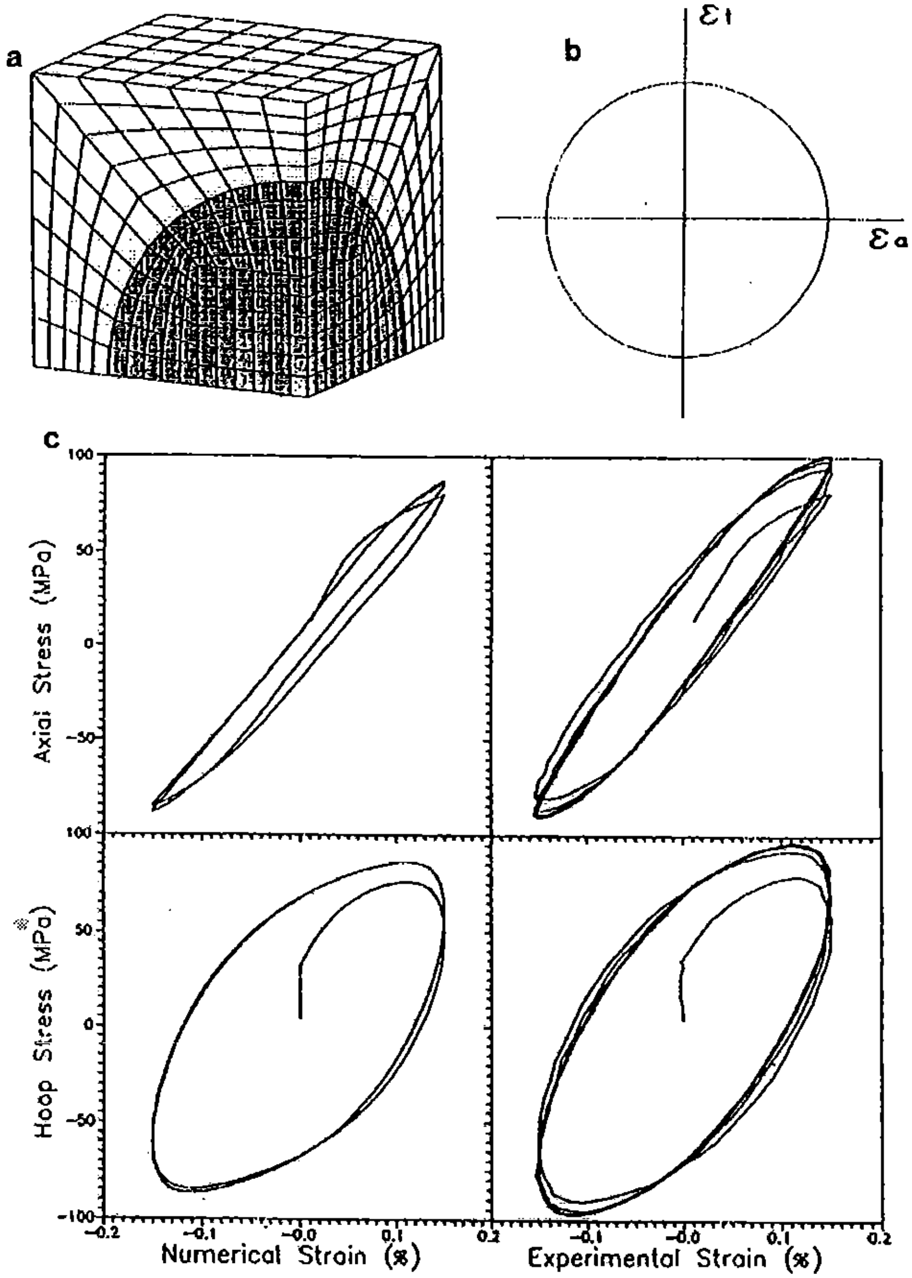

Fig. 6. Response of 6061 aluminium alloy reinforced with 20% volume fraction of alumina particles subjected to a 90° out-of-phase cyclic load.
a: finite element model in the calculation; b: applied cyclic strain path;
c: comparison of experimental and numerical results.

Monotonic loading with different strain rates and with abrupt changes in strain-rate

In Fig. 7b, the monotonic test results of annealed type 304 stainless steel under three different strain-rates are presented[15]. For the two slow rates, there were abrupt jumps in the strain-rate at specified strains, see fig. 7b. The model predictions are shown in Fig. 7a, which are in good agreement with the experimental data.. In addition, a predicted stress-strain curve under a *constant stress-rate* is also presented in the figure. It is to be noted that in the latter case the strain-rate would not have a constant value once the material enters the plastic regime. Due to the change in strain-rate, the uniaxial curve under a constant stress-rate usually has a more gradual transition from the elastic to plastic response (c.f. Fig. 7a).

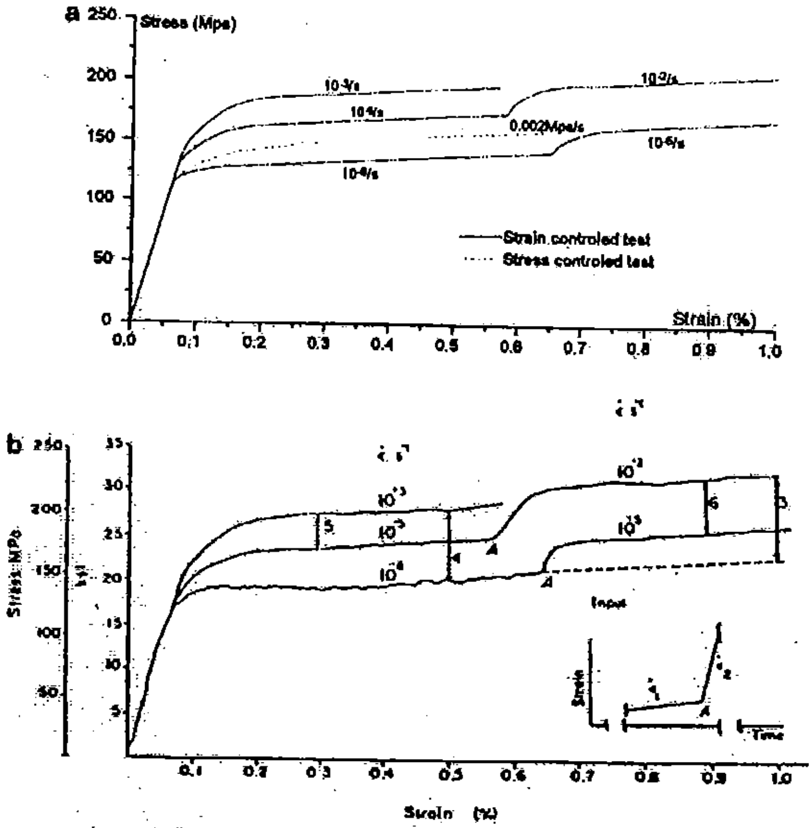

Fig. 7. Uniaxial stress-strain curves of 304 stainless steel at different strai rates. a: predicted results; b: test results, after Krempl et al [15]

Effect of rate and rate-history on strain-hardening

Uniaxial cyclic tests comprised of three levels of strain-rates applied in predetermined sequences were performed on specimens of type 304 stainless steel [16]. The imposed strain amplitude was 0.003 with strain rate ranging from 6×10^{-3} to 6×10^{-4} to 6×10^{-5} s^{-1}. At each strain-rate level, 50 cycles were applied before switching to another rate to ensure stable material response. Fig. 8 shows relations between the stress amplitude and number of cycles of three uniaxial cyclic tests with different strain-rate histories. The stable stress-strain loops of these tests at each strain-rate are depicted in Fig. 9a. For the test with decreasing sequence of strain-rates, F-M-S, we observe a decrease in the stress amplitude with decreasing strain-rate. However, no appreciable change is observed in the test with increasing sequence, S-M-F. These results show the effect of strain-rate history on the strain-hardening behaviour of the material. The predicted stress-strain loops for the three uniaxial cyclic tests are shown in Fig. 9b.

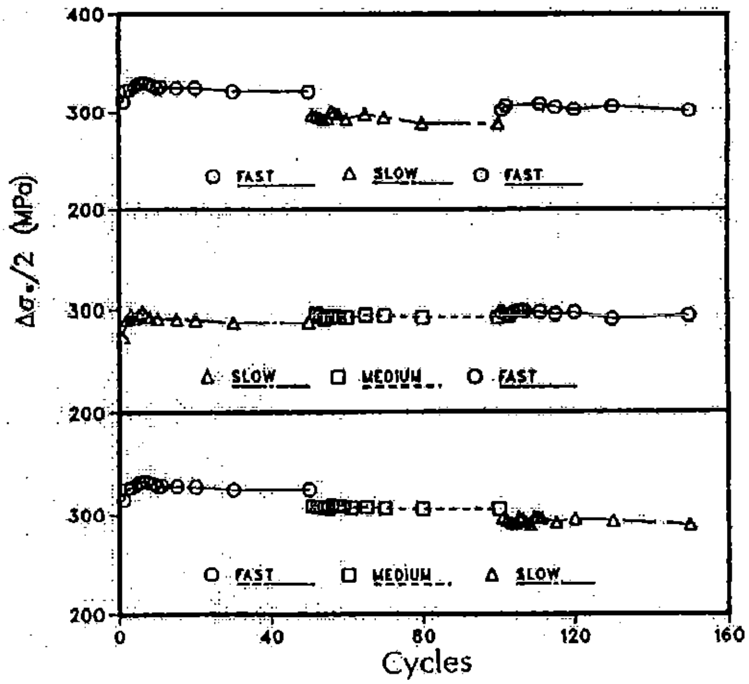

Fig. 8. Stress amplitude versus number of cycles for uniaxial cyclic tests.

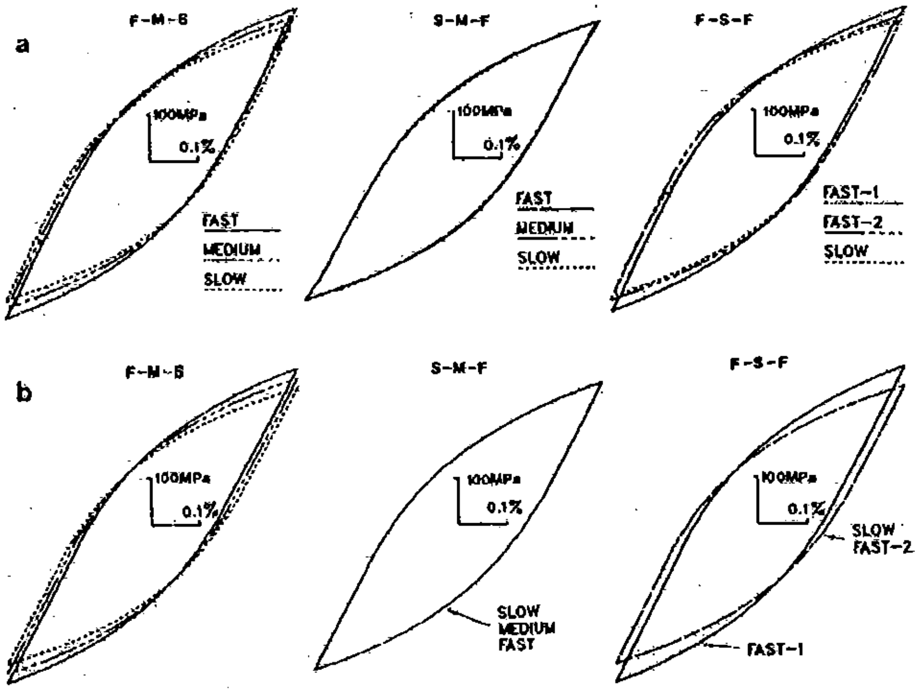

Fig. 9. The stable stress-strain loops at each step of strain-rate for the uniaxial cyclic tests. a: test results; b: predicted results.

Conclusions

An elastoplastic constitutive model has been developed and implemented into the user-supplied material model of the FEM code ADINA. The model has the following features:

(1) The constitutive models is a comprehensive one yet relatively simple to implement. The input data of the model can be easily determined from simple experiments.

(2) It distinguishes two types of plastic loading by the introduction of the stress memory surface and as such the model is particularly suitable for predicting materials' behaviour under complex cyclic loading and ratcheting strain accumulation.

(3) The developed subroutines of this constitutive model and the resulting finite element code has been used to predict various materials' behaviour as well as the structural response.

References

[1] Prager, W. (1955), "The theory of plasticity - a survey of recent achievements", Proceedings of the Institute of Mechanical Engineers, vol. 169, pp. 41-57.

[2] Ziegler, H., (1959), "A modification of Prager's hardening rule", Quarterly of Applied Mathematics, vol. 17, pp. 55-65.

[3] Mroz, Z., (1967), "An attempt to describe the behaviour of metals under cyclic loads using a more general work hardening model", Acta Mech., vol. 7, pp. 199-212.

[4] Ellyin F., (1988), "Recent developments in predicting multiaxial fatigue failure", Res Mechanica, vol. 25, pp. 1-23.

[5] Ellyin, F. and Xia, Z., (1995), "A new elasto-plastic constitutive model inserted into the user-supplied material model of ADINA", Computers and Structures, vol. 56, pp. 283-294.

[6] Ellyin, F. and Xia, Z., (1991), "A rate-dependent inelastic constitutive model, part I: elastic-plastic flow", ASME J. Engng. Mater. Technol. vol. 113, pp. 314-323

[7] Xia, Z. and Ellyin, F., (1995), "A finite elastoplastic constitutive formulation with new co-rotational stress-rate and strain hardening rule", ASME J. Appl. Mech., vol. 62, pp. 733-739.

[8] Phillips, A., (1986), "A review of quasistatic experimental plasticity and viscoplasticity", Int. J. Plasticity, vol. 2, pp. 315-328.

[9] Xia, Z. and Ellyin, F., (1997), "A constitutive model with capability to simulate complex multiaxial ratcheting behaviour of materials", Int. J. Plasticity, in press.

[10] Xia, Z. and Ellyin, F., (1991), "A rate-dependent inelastic constitutive model, part II: Creep deformation including prior plastic strain effects", ASME J. Engng. Mater. Technol. vol. 113, pp. 324-328.

[11] McDowell, D.L., (1985), "A two surface model for transient nonproportional cyclic plasticity, Part 1 & 2", ASME J. Appl. Mech., vol. 52, pp. 298-308.

[12] Xia, Z. and Ellyin, F. (1991), "Nonproportional multiaxial cyclic loading: experiments and constitutive modeling", ASME J. Appl. Mech, vol. 113, pp.317-325

[13] Jiang, Y. and Sehitoglu, H., (1994), "Cyclic ratcheting of 1070 steel under multiaxial stress state", Int. J. Plasticity, vol. 10, pp. 579-608.

[14] Meijer, G., Xia, Z. and Ellyin, F. (1997), "Biaxial cyclic analysis of Al_2O_{3p}©6061 Al composite", Acta Materialia, in press.

[15] Krempl, E. and Kallianpur, V. V., (1984), "Some critical uniaxial experiments for viscoplasticity at room temperature", J. mech. phys. solids, vol. 32, pp. 301-314.

[16] Ellyin, F. Xia, Z. and Sasaki, K. (1993), "Effect of rate and rate history on plastic deformation: experiments and constitutive modeling", Int plasticity, vol. 9, pp. 951-959.